Controllable embedding of size-selected copper nanoparticles into polymer films

Bonde, Hans Christian; Fojan, Peter; Popok, Vladimir N.

Published in:
Plasma Processes and Polymers

DOI (link to publication from Publisher):
10.1002/ppap.201900237

Publication date:
2020

Document Version
Accepted author manuscript, peer reviewed version

DOI: 10.1002/ppap.201900237
FULL PAPER

Controllable embedding of size-selected copper nanoparticles into polymer films

Hans Christian Bonde, Peter Fojan, Vladimir N. Popok *

_____

Department of Materials and Production, Aalborg University, Aalborg, Denmark

Correspondense
Vladimir Popok, Department of Materials and Production, Aalborg University, Skjernvej 4A, 9220 Aalborg, Denmark
E-mail: vp@mp.aau.dk

_____

Abstract

An ability to control the extent of metal nanoparticle (NP) embedding into polymer films attracts attention for applications in a few research brunches. In this work, the behaviour of size-selected copper NPs produced by gas aggregation method and deposited on poly(methyl methacrylate) and polystyrene films is studied under a thermal annealing above and below the glass transition temperature. Several important tendencies of the embedding dynamics in dependence on NP size, annealing temperature and time as well as type of polymer are found and analysed. The physical models explaining the particle behaviour and allowing to elaborate practical recommendation on controllable embedding of metal NPs into polymer films are suggested.

Keywords: gas-aggregated metal nanoparticles; nanoparticle embedding; polymer films; thermal annealing

1 Introduction

Incorporation of metal nanoparticles (NPs) into polymer films has been attracting attention for the last couple of decades motivated by applications in electronics, optics, sensing and microwave technologies as well as in biological and medical branches [1-5]. In many practical cases, for example, for sensing, antibacterial purposes and plasmonic applications, there is an interest to control the extent of NP embedding. This ensures, on the one hand, that a certain fraction of the particle surface is open for an external interaction and, on the other hand, that the NP, partly embedded into a polymer, is protected against removal from the surface through following treatments [6]. Formation of polymer composites with metal NPs can be achieved by different *in situ* and *ex situ* methods [7, 8]. Although *in situ* approaches are effective in control of particle filling factor in a matrix [9-12], they do not allow to tune the extent of NP embedding. Thus, an alternative is *ex situ* particle formation and following embedding into a polymer. NPs can be produced either by chemical or physical means [1, 2, 13, 14]. Among the physical approaches, gas aggregation cluster technique attracts considerable attention enabling (i) to produce very pure monocrystalline metal NPs as well as alloy or compound aggregates with tuneable composition and structure; (ii) to provide selection of NP sizes (masses) and kinetic energy tuning to adjust the cluster-surface interaction mechanism; (iii) to perform surface patterning with NPs [15-17]. The experiments on metal cluster implantation into polymers showed that the NPs became fully embedded even at very low kinetic energies [18, 19]. Thus, the alternative option is NP soft landing on a polymer followed by specific treatment facilitating particle embedding [1, 5].

From surface science, it is well known that a rigid metal particle on a surface of soft material, for example, a polymer, would have a tendency for immersion to minimize tension at the interface [20, 21] due to a large difference in surface energy between metals (typically above 1000 mJ/m^2) [22] and polymers (typically below 100 mJ/m^2) [23, 24]. However, NP embedding into a solid state polymer requires creation of a void (indentation). In other words, the Gibbs

free energy of the system must be changed promoting work of adhesion. This energy can be supplied by external heating at temperatures close to or above the glass transition point (T_g) leading to an increase of polymer chain flexibility and facilitating the indentation [25].

This strategy was successfully tested and the studies have revealed a number of practical issues related to metal NP embedding into polymers: a few nm thick surface layer of a polymer is characterised by higher molecular mobility and lower T_g compared to the bulk [26], thus, affecting the NP immersion; embedding can start at temperatures below T_g [27, 28]. It can also occur through wetting of a particle surface by an ultrathin polymer layer in the case of molten polymer [29]. However, the state-of-the-art on the NP/polymer interaction indicates a significant discrepancy regarding particle embedding dynamics. A slow (on a scale of hours) embedding of silver and gold NPs into poly(methyl methacrylate) (PMMA) and polystyrene (PS) under annealing at temperatures above T_g is reported in [24]. In this case, the NPs were formed by self-aggregation after metal evaporation, thus, representing a variety of sizes and shapes. Other studies reported a much shorter (minute scale) immersion time for gold, silver and copper NPs into the same type of polymers, PMMA and PS [21, 27, 30, 31]. In these works, NPs of defined sizes were used, hence, leading to the assumption that the particle size matters.

In the current work, we utilise Magnetron Sputtering Cluster Apparatus (MaSCA) [30] for formation of Cu NPs, their mass filtering followed by soft-landing on PMMA and PS films prepared by a standard spin-coating procedure. Dynamics of particle immersion is studied using atomic force microscopy (AFM) after each annealing stage performed at temperatures either below or above T_g.

2 Experimental Section

Si substrates coated with a polymer film are produced by a standard spin coating method using solutions of 1.5% PMMA in chlorobenzene and 2% PS in toluene. Molecular weight M_w of used PMMA is 950000 g/mol and of PS is 192000g/mol. To ensure that no residual solvent left

in the films and to allow the polymer chains to relax, the samples are heated at 120 ℃ (above T_g, see more details below) for 30 min. The spin coating parameters are adjusted to obtain films of the same thickness for both polymers, which is found by ellipsometry to be ≈110 nm.

An important issue for the current study is defining the glass transition points for PMMA and PS. It is known that T_g depends on the M_w of polymers and it can also vary with the film thickness when coming to the nanoscale. Earlier studies showed T_g to be 111±1 and 105±1 ^oC for PMMA and PS, respectively, with M_w comparable to that used in the current study [32, 33]. It was also found that with decreasing the polymer film thickness a high anisotropy decay was initiated at lower temperatures compared to bulk polymers; molecules reorient more rapidly in thinner films affecting T_g [34]. However, this effect is noticeable only for the films thinner than 100 nm. Since our films are thicker, we can assume that the above-mentioned bulk temperatures are still valid.

Copper NPs are produced using a commercial nanocluster source (NC200U from Oxford Applied Research) attached to a home-built vacuum setup, which is called MaSCA. More details about the system and typical operation parameters of the source can be found elsewhere [30, 35]. In the current experiments, a Cu target of 99.99% purity in shape of a disk (50 mm in diameter) is used for the NP formation.

One of the key parts of MaSCA is an electrostatic quadrupole mass selector (EQMS) [36] allowing size-selection (mass-filtering) of NPs, which are produced in a range of sizes in the source. The filtering is based on deflection of a charged particle trajectory in an electrostatic field. Thus, only NPs of a certain mass-to-charge ratio can pass through the EQMS under a given applied potential [36]. For particles carrying unit charge, the EQMS filters a certain mass. However, if the charge is equal to 2 or 3, then, respectively, the NPs of double and triple masses will be selected under the same applied potential. Recent studies have shown that the ratio of highly-charged NPs with respect to singly-charged ones can vary between 10-18% for low selecting potential of 200V, while it increases to almost 30 % for a potential value of 1100 V

[35]. In the current study, the NPs are filtered under two potentials of 200 and 1200 V at the field configuration selecting negatively charged particles, which are then soft-landed on the spin coated PMMA and PS films. Surface coverage of samples by NPs slightly varies from sample to sample but, for all cases, it is chosen to be low in order to avoid/minimize an interaction of the individual NPs.

Only NPs of the most abundant size (mass), i.e. singly charged ones, are monitored by atomic force microscopy (AFM). These measurements are carried out in tapping mode utilizing Nanolaboratory Ntegra-Aura (NT-MDT) and using standard commercial Si cantilevers with a force constant of 3-6 N/m and a tip curvature radius of ≤ 10 nm.

Embedding of NPs into the polymer films is provided by thermal annealing at temperatures of either 85 or 125 °C, i.e. below or above T_g for both polymers. The samples are heated on a hotplate in ambient air during time intervals spanning from 1 to 60 minutes. After each annealing step, the NP height is measured by AFM. The scans are always carried out for the same areas, i.e. immersion of individual particles is monitored as a function of annealing steps (annealing time). In order to find these areas, a cross is produced by focused ion beam milling on every Si substrate used for the polymer film spin coating.

3 Results

Using AFM, heights of as-deposited NPs selected at voltages of 200 and 1200 V are measured on both types of polymer films (see Tab. 1). Further, these particles will be referred to as small and large, respectively. Under the assumption that the NPs keep an almost spherical shape after deposition on the samples (the particles are just slightly oblate [36, 37]), the height is considered to be approximately equal to the diameter *d*. Hence, we can use the values of Tab. 1 as references for estimation of the embedding ratio of NPs after annealing. One should also take into account that the roughness of the polymer films affects the measurements especially when

the particles become almost fully embedded. Root mean square values of 0.5 nm and 0.6 nm are found for PMMA and PS, respectively, for areas of 2×2 μm^2.

Table 1. Heights with standard deviations of Cu NPs size-selected at 200 and 1200 V and deposited on PMMA and PS

Type of polymer	**Height (at 200V) [nm]**	**Statistics* (at 200 V) [#]**	**Height (at 1200 V) [nm]**	**Statistics* (at 1200 V) [#]**
PMMA	13.4±1.3	53	18.0±3.0	80
PS	13.0±1.2	83	19.3±3.0	66

* Statistics is a number of NPs used for the height estimation

AFM images of as deposited small NPs are shown in Fig. 1a and Fig. 2a for PMMA and PS, respectively. Panels (b) and (c) in both figures show examples of annealed samples. The NPs are numbered in order to make it easier for the reader to follow the embedding by comparing the as-deposited case with following annealing stages. The embedding dynamics for all samples under the study is presented in Figs. 3-6 as dependencies of NP height on the annealing time. For the annealed samples, the height is averaged over 40-50 particles. It is worth noting that earlier studies of the silver NPs on PMMA have shown that annealing leads to the NP embedding without any major changes of the shape [21]. From the images presented in Figs. 1 and 2 one can see that the NPs do not have tendency to move across the surface or aggregate under the annealing.

The small NPs on PMMA annealed below T_g (PMMA1) show no embedding during the first two minutes and then an immersion for approximately 3 nm during the next few minutes (see insert in Fig. 3). The following annealing leads to gradual embedding with time. The NPs stabilise after 148 min at a level corresponding to approximately 0.4*d* above the surface. When annealed above T_g, the small NPs show very fast immersion (PMMA2 in Fig. 3). After 3 min they are embedded to an extent where it is hard to distinguish between NPs slightly towered

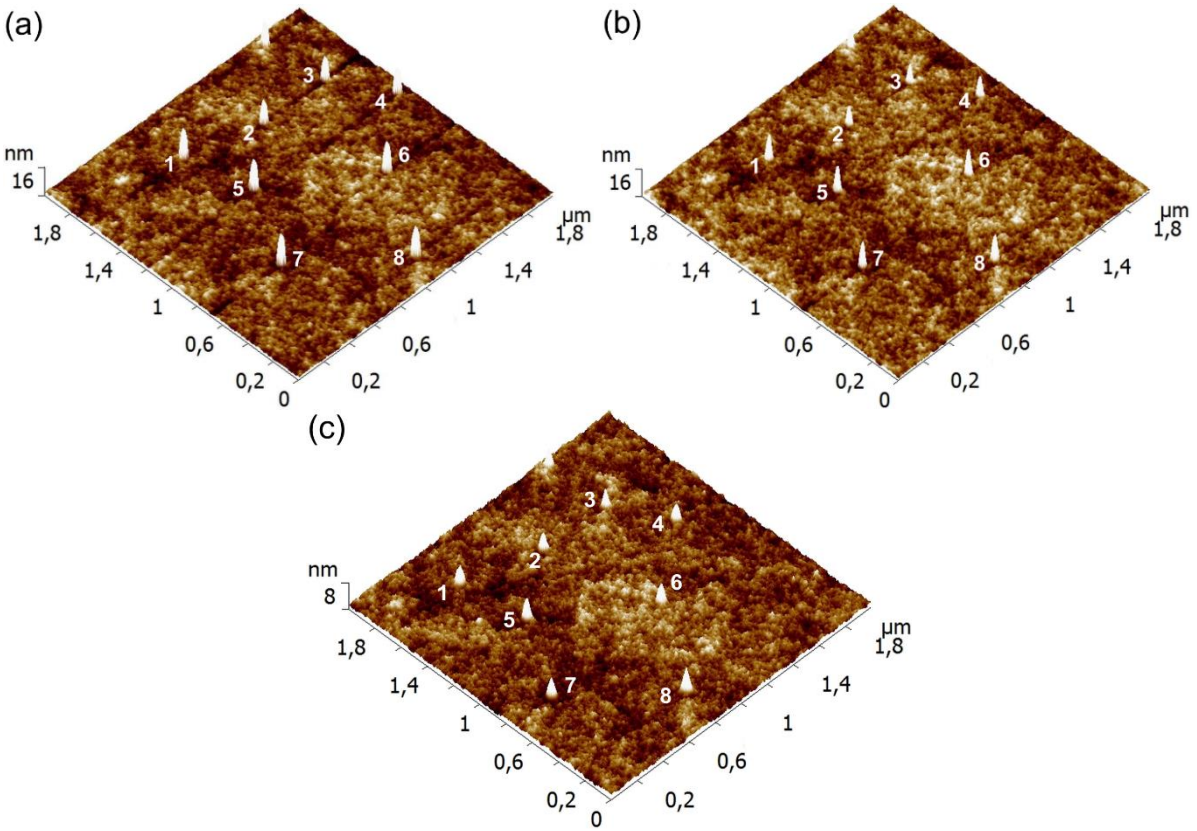

Figure 1. AFM images of small Cu NPs on PMMA (a) as-deposited, after annealing at 85 °C for (b) 4 min and (c) 208 min. Individual NPs are numbered in order to better visualise the embedding with annealing time.

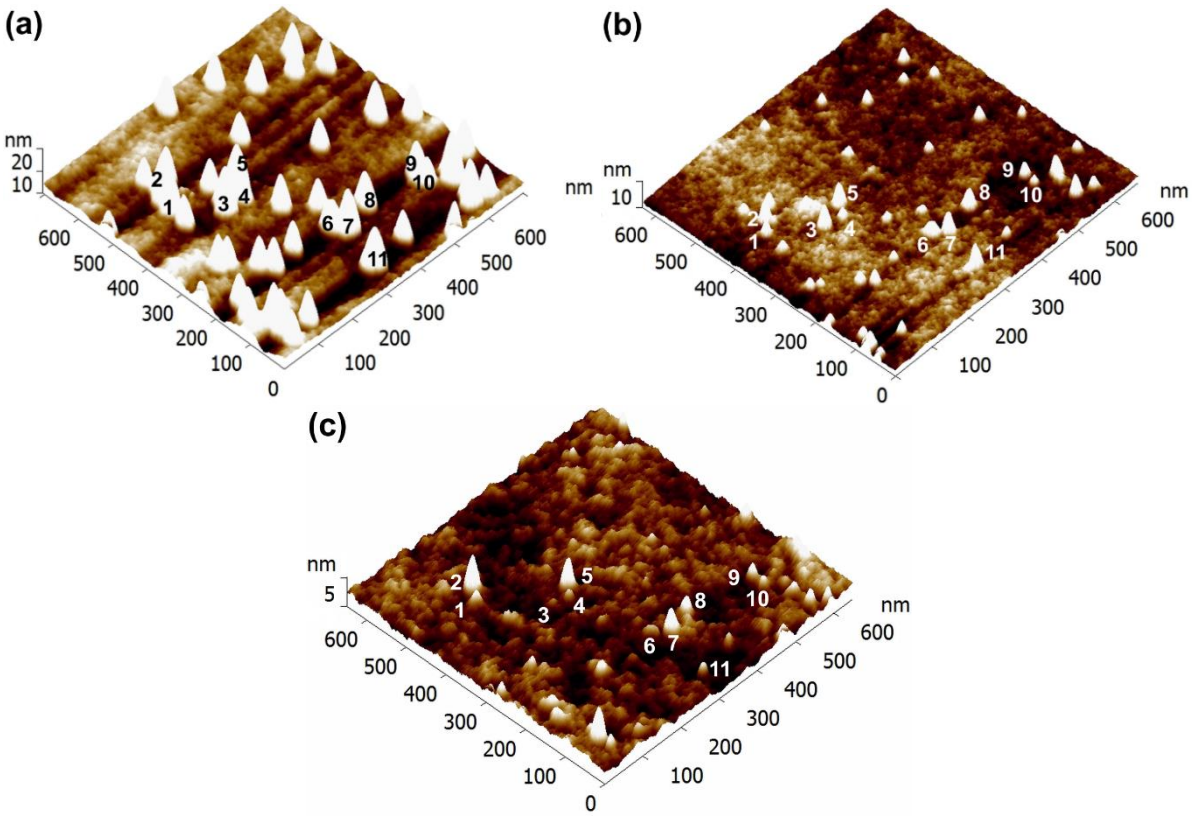

Figure 2. AFM images of small Cu NPs on PS (a) as-deposited, after annealing at 125 °C for (b) 7 min and (c) 202 min. Some NPs are numbered in order to better visualise the embedding with annealing time.

above the surface and bumps on the polymer surface. Longer annealing does not lead to any further changes as can be seen in Fig. 3.

The large NPs deposited on PMMA and annealed below T_g (PMMA3 in Fig. 4) show a very similar behaviour to that of the small NPs for the first few minutes of annealing: they do not immerse (see insert in Fig. 4). However, contrary to the small NPs, we observe a very low degree of embedding (only 1-2 nm) even for long annealing times; NPs stabilise. The large NPs annealed above T_g (PMMA4 in Fig. 4), on the other hand, show a fast immersion into the polymer within the first 2 min (see insert in Fig. 4), i.e. similar behaviour to that of the small NPs. However, the degree of immersion is lower; the particles are for about 0.55d above the surface. The following annealing steps lead to further gradual immersion and after 95 min the NPs stabilise at about 0.4d above the surface as can be seen in Fig. 4.

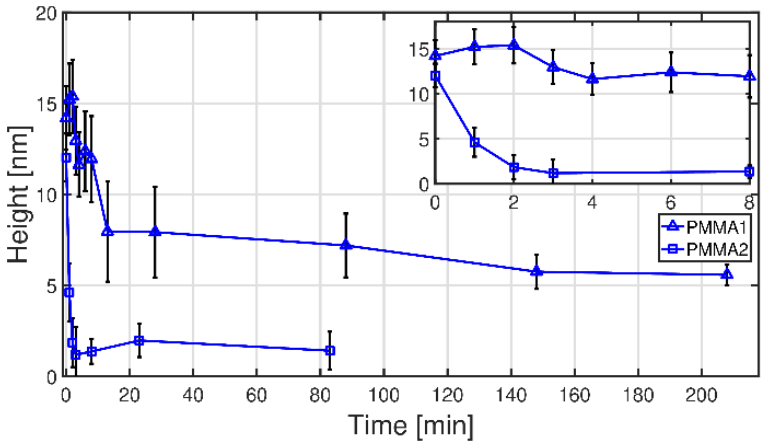

Figure 3. Mean height vs annealing time for small NPs on PMMA treated at temperatures below T_g (PMMA1) and above T_g (PMMA2). The error bars show standard deviations.

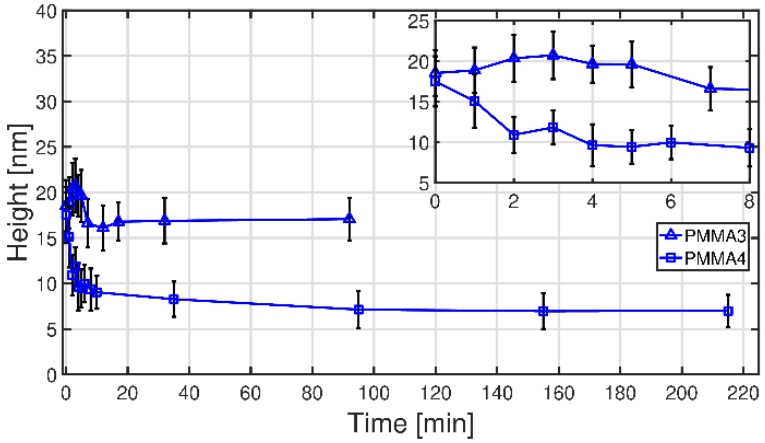

Figure 4. Mean height vs annealing time for large NPs on PMMA treated at temperatures below T_g (PMMA3) and above T_g (PMMA4). The error bars show standard deviations.

The PS sample with small NPs annealed below T_g (PS1) shows a slow and only partial immersion as can be seen in Fig. 5. After 202 min of annealing, the NPs seem to stabilise at a level of around 0.5*d* above the surface, i.e. showing the same dynamics as the small particles on PMMA. The annealing above T_g (PS2) shows initial NP immersion to a level of 0.3*d* above the surface within the first 2 min. Then, the embedding process slows down and gradually leads to almost full embedding after 202 min, as can be seen in Fig. 5, when the height is comparable to the roughness of the polymer surface. Comparing this case to PMMA, one can point out a bit slower initial embedding but the NPs reach the same final conditions on a long time scale.

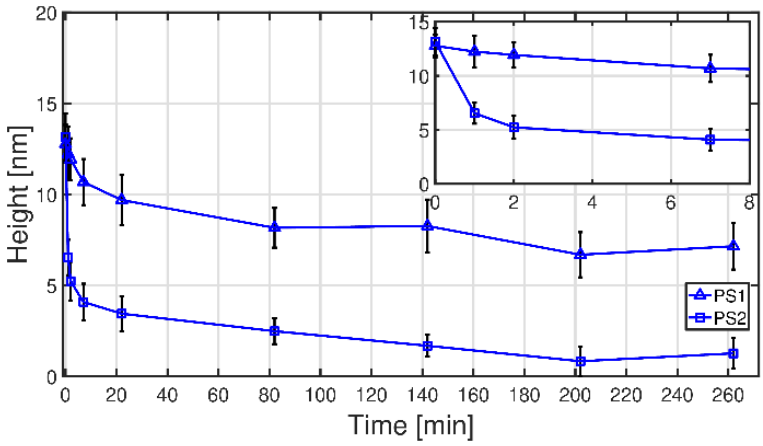

Figure 5. Mean height vs annealing time for small NPs on PS treated at temperatures below T_g (PS1) and above T_g (PS2). The error bars show standard deviations.

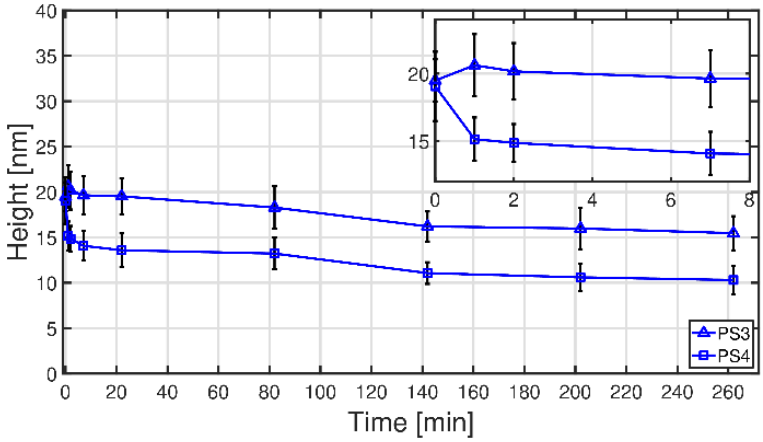

Figure 6. Mean height vs annealing time for large NPs on PS treated at temperatures below T_g (PS3) and above T_g (PS4). The error bars show standard deviations.

Fig. 6 shows the embedding dynamics of the large NPs on PS annealed below and above T_g, PS3 and PS4, respectively. For both samples, we observe the time-dependence of

embedding to be similar to the cases of PMMA with the large NPs. However, we also see some differences. It requires longer annealing times for PS to stabilise the particles. For the thermal treatment below T_g (PS4), the NPs become embedded to a level of 0.6*d* above the surface while in the case of PMMA it is about 0.4*d*.

4 Discussion

Summarising the above-described dependencies, we can distinguish a few important tendencies.

Annealing at $T > T_g$ leads to fast (on a scale of a few minutes) high extent embedding of the NPs: only a little fraction of the small ones towers above the surface; the large NPs penetrate less deep but still significant. This behaviour agrees well with a number of early studies discussed in the Introduction [21, 27, 30, 31]. The minute-scale annealing times above the glass transition temperature are sufficient to provide the change of Gibbs free energy required for void formation and NP indentation.

The second observed tendency is related to the treatments at $T < T_g$. In these cases, the NPs demonstrate a shallow immersion. The small particles become embedded for 5-7 nm, the large ones for 2-4 nm into PMMA and PS. This shallow immersion can be explained by higher molecular mobility and lower T_g in the thin near surface layers compared to the bulk [26, 27]. For PS, the thickness of a "liquid-like" surface layer was found to be 3-4 nm [26]. In [38], it was shown that the gold NP embedding into PS is localised to about 5 nm thick surface layer under the thermal treatment at temperatures below T_g. These thickness values agree well with our observations.

One more important finding to be emphasised is that the particle size matters. Faster and deeper immersion of the small particles compared to the large ones for both annealing conditions (below and above T_g) is observed; the small particles become fully or almost fully embedded. This observation is in good agreement with the earlier studies showing a high extent

of embedding for ≤ 10 nm gold, silver and copper NPs into PS, polyimide and some other polymers [26, 28, 39]. However, larger particles do not undergo full embedment. We found a good correlation of our results with the ones for 20 nm gold particles on PS, which stabilise at a height of 5 nm above the surface after 100 min of annealing above T_g and do not immerse deeper even after a few thousand minutes of thermal treatment [38].

It is known from literature that a metal NP becomes embedded into a polymer under the conditions when the surface tension at the NP/air interface γ_{NP} is greater than the sum of the surface tensions at the polymer/air γ_P and NP/polymer $\gamma_{NP/P}$ interfaces [20]

$$\gamma_{NP} > \gamma_P + \gamma_{NP/P}. \quad (1)$$

Considering the projection of surface tensions on a tangent to the particle surface (see Fig. 7a), one obtains the following equation

$$\gamma_{NP} > \gamma_{NP/P} - \gamma_P \cos\varphi, \quad (2)$$

where the direction of force related to γ_P supports the embedding until $\varphi < 90^o$. With increasing immersion depth, $\cos\varphi$ becomes negative (see Fig. 7b) that leads to the increase of right side of eq. (2). At some point we can come to an equality

$$\gamma_{NP} = \gamma_{NP/P} - \gamma_P \cos\varphi. \quad (3)$$

This is an equilibrium condition when the free energy of the system reaches zero and the NP stops immersing. By considering the geometry shown in Fig. 7b, one can derive a simple equation relating the height of the particle towered above the surface h to the particle radius r

$$h = r(1+\cos\varphi). \quad (4)$$

Assuming the same equilibrium conditions for the small and large NPs (same value of $\cos\varphi$), one should expect a higher h value for particles with larger radius, which is the case observed in the experiments.

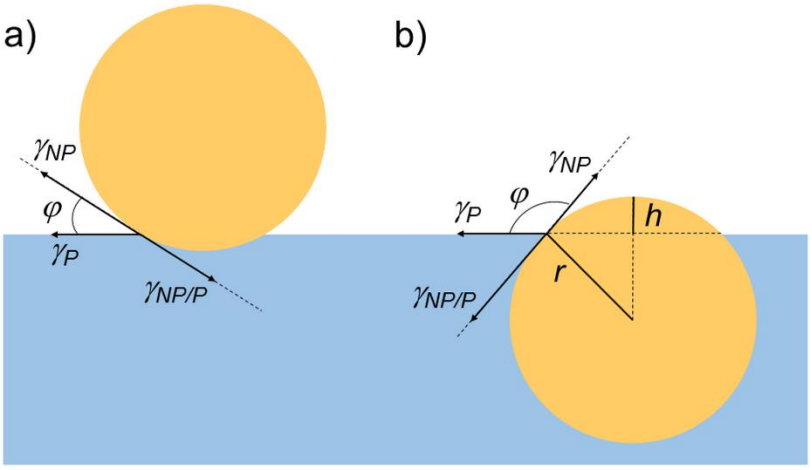

Figure 7. Schematic picture of rigid particle embedding into soft substrate: a) beginning of the process and b) stabilisation. See text for details.

It is worth mentioning that the above-presented model is a simplification, which assumes a NP embedding into a bulk and it does not take into account any specific phenomena related to the properties of particular polymers, film thickness, deposition regime and NP-NP interactions [40-42]. For instance, lower M_w of the polymer would cause higher NP mobility. However, we observe a tendency that the NPs become embedded into PMMA a bit faster and deeper than into PS at $T > T_g$ despite M_w of PMMA is higher than that of PS in our case. The observed tendency might be related to some differences in heat dissipation or molecular properties, for instance, lower mobility of PS chains containing benzene rings. This issue requires further investigation.

Polymer film thickness is another important parameter. It is known that the polymer chain mobility increases and the glass transition temperature decreases for the films with lower thickness [34], thus, affecting the work of adhesion required for the NP embedding. However, the PMMA and PS films used in the current study are thick enough to resemble bulk polymers [34]. For ultra-thin polymer films, when the particle diameter is comparable with the thickness, van der Waals interaction of NPs with underlying substrates also plays a role [41]. In our case, the interaction energy with the Si substrate calculated using the approach suggested in [41] is found to be negligibly small. We can also disregard contribution of van der Waals interaction

between the NPs because the particles are deposited in a low-coverage regime and they are sufficiently far from each other.

One more important issue to be mentioned, when discussing the embedding dynamics, is a copper NP oxidation. It is known that coper is a relatively high-reactive metal, which is tended to form predominantly Cu_2O when kept at room temperature in the ambient atmosphere [43, 44]. For the case of copper NPs kept at room temperature, the oxide formation was found to be a slow process yielding a 3-5 nm thick shell after three weeks [45]. However, under annealing, one can expect faster oxide growth especially on the NP top parts towered above the surface, thus, affecting the embedding. Surface energy of Cu_2O is around 55 mJ/m^2 [46], which is comparable with those of PMMA and PS (30-40 mJ/m^2) [24]. Hence, an oxidised copper NP would lose the driving force for the immersion. This could be the reason why we do not observe 100% embedding of the NPs under the annealing above the glass transition point.

5 Conclusion

In the current work, embedding dynamics of size-selected copper NPs (with mean sizes of approximately 13 and 18-19 nm) into PMMA and PS films under thermal annealing above and below the glass transition temperature is studied.

The obtained results reveal a few practically important dependences:

(i) The annealing at $T > T_g$ causes a high extent of embedding of the NPs into both polymers. The process is characterised by an initial stage of fast and high-rate embedding which is followed by slow and low-rate immersion until stabilisation of the NPs. It can be concluded that the minute-scale annealing above the glass transition temperature is sufficient to provide the change of Gibbs free energy required for initial void formation and NP indentation into a polymer film. The particles undergo almost full embedding into the polymers. Towering of a small NP fraction above the surface can be related to the oxidation.

(ii) The annealing at $T < T_g$ leads to only shallow (a few nm deep) embedding into the near surface polymer layer which is characterised by higher molecular mobility and lower glass transition point compared to the bulk facilitating the partial particle penetration.

(iii) It is found that the embedding dynamics depends on particle size. Smaller particles become embedded faster and deeper. This tendency can be explained using considerations of the surface tension and change in the Gibbs free energy of the particle/polymer system.

(iv) There are week differences between the embedding into PMMA and PS. It is observed that the NPs become embedded into PMMA a bit faster and deeper than into PS at $T > T_g$. This tendency is not clear and requires further investigation.

Acknowledgements: We would like to acknowledge contribution of M. K. Sandager, C. Olesen and S. Scheele (Aalborg University) to the AFM measurements.

REFERENCES

[1] J. Prakash, J.C. Pivin, H.C. Swart, *Adv. Coll. Interface Sci.* **2015**, *226*, 187.

[2] F. Faupel, V. Zaporojtchenko, T. Strunskus, M. Elbahri, *Adv. Eng. Mater.* **2010**, *12*, 1177.

[3] O.M. Folarin, E.R. Sadiku, A. Maity, *Int. J. Phys. Sci.* **2011**, *6*, 4869.

[4] Y. Zare, I. Shabani, *Mater. Sci. Eng. C* **2016**, *60*, 195.

[5] V.N. Popok, in *Polymer-based Multifunctional Nanocomposites and Their Applications*, (Eds. K. Song, C. Liu and J.Z. Guo), Elsevier, Amsterdam **2019**, Ch. 2, P. 35.

[6] M. Hanif, R.R. Juluri, P. Fojan, V.N. Popok, *Biointerface Res. Appl. Chem.* **2016**, *6*, 1564.

[7] S. Li, M.M. Lin, M.S. Toprak, D.K. Kim, M. Muhammed, *Nano Rev.* **2010**, *1*, 5214.

[8] V. Torrisi, F. Ruffino, *Coatings* **2015**, *5*, 378.

[9] R.I. Khaibullin, V.N. Popok, V.V. Bazarov, E.P. Zheglov, B.Z. Rameev, C. Okay, L.R. Tagirov, B. Aktas, *Nucl. Instr. Meth. Phys. Res. B* **2002**, *191*, 810.

[10] V.N. Popok, in *Radiation Effects in Polymeric Materials*, (Eds. V. Kumar, B. Chaudhary, V. Sharma, K. Verma), Springer Nature, **2019**, P. 66.

[11] T. Hanemann, D.V. Szabo, *Materials* **2010**, *3*, 3468.

[12] S. Porel, S. Singh, S.S. Harsha, D.N. Rao, T.P. Radhakrishnan, *Chem. Mater.* **2005**, *17*, 9.

[13] L. Tröger, H. Hünnefeld, S. Nunes, M. Oehring, D. Fritsch, *J. Phys. Chem. B* **1997**, *101*, 1279.

[14] S. Li, J. Qin, A. Fornara, M. Toprak, M. Muhammed, D.K. Kim, *Nanotechnol.* **2009**, *20*, 185607.

[15] W.A. de Heer, *Rev. Mod. Phys.* **1993**, *65*, 611.

[16] I.M. Goldby, B. von Issendorf, L. Kuipers, R.E. Palmer, *Rev. Sci. Instrum.* **1997**, *68*, 3327.

[17] V.N. Popok, E.E.B. Campbell, *Beams of atomic clusters: effects on impact with solids, Rev. Adv. Mater. Res.* **2006**, *11*, 19.

[18] L. Ravagnan, G. Divitini, S. Rebasti, M. Marelli, P. Piseri, P. Milani, *J. Phys. D: Appl. Phys.* **2009**, *42*, 082002.

[19] C. Ghisleri, F. Borghi, L. Ravagnan, A. Podests, C. Melis, L. Colombo, P. Milani, *J. Phys. D: Appl. Phys.* **2014**, *45*, 015301.

[20] G.J. Kovacs, P.S. Vincett, *Thin Sol. Films* **1984**, *111*, 65.

[21] M. Hanif, R.R. Juluri, M. Chirumamilla, V.N. Popok, *J. Polym. Sci. B: Polymer Phys.* **2016**, *54*, 1152.

[22] F. Aqra, A. Ayyad, *Appl. Surf. Sci.* **2014**, *314*, 308.

[23] Yu. Lipatov, A. Feinermann, *Adv. Colloid Interface Sci.* **1979**, *11*, 195.

[24] F. Ruffino, V. Torrisi, G. Marletta, M.G. Grimaldi, *Appl. Phys. A* **2012**, *107*, 669.

[25] J. Erichsen, J. Kanzow, U. Schurmann, K. Dolgner, K. Gunter-Schade, T. Strunskus, V. Zaporojtchenko, F. Faupel, *Micromol.* **2004**, *37*, 1831.

[26] J.H. Teichroeb, J.A. Forrest, *Phys. Rev. Lett.* **2003**, *91*, 016104.

[27] R. Weber, I. Grotkopp, J. Stettner, M. Tolan, W. Press, *Macromol.* **2003**, *36*, 9100.

[28] S. Hajati, V. Zaporojtchenko, F. Faupel, S. Tougaard, *Surf. Sci.* **2007**, *601*, 3261.

[29] R.D. Deshmukh, R.J. Composto, *Langmuir* **2007**, *23*, 13169.

[30] V.N. Popok, M. Hanif, F.A. Ceynowa, P. Foyan, *Nucl. Instrum. Meth. Phys. Res. B* **2017**, 409, 91.

[31] F.A. Ceynowa, M. Chirumamilla, V.A. Zenin, V.N. Popok, *MRS Advances* **2018**, *3(45-46)*, 2771.

[32] A.M. Bowles, *Stress Evolution in Thin Films of a Polymer*, PhD thesis, Harvard University, **2006**.

[33] *Hitachi High-Tech Application Notes: Thermal Analysis* **1995**, *68* https://www.hitachi-hightech.com/file/global/pdf/products/science/appli/ana/thermal/application_TA_068e.pdf

[34] K. Paeng, R. Richert, M.D. Ediger, *Soft Matter* **2012**, *8*, 819.

[35] V.N. Popok, L. Gurevich, *J. Nanopart. Res.* **2019**, *21*, 171.

[36] H. Hartmann, V.N. Popok, I. Barke, V. von Oeynhausen, K.-H. Meiwes-Broer, *Rev. Sci. Instrum.* **2012**, *83*, 073304.

[37] S.M. Novikov, V.N. Popok, A.B. Evlyukhin, M. Hanif, P. Morgen, J. Fiutowski, J. Beermann, H.-G. Rubahn, S.I. Bozhevolnyi, *Langmuir* **2017**, *33*, 6062.

[38] D. Qi, M. Ilton, J.A. Forrest, *Eur. Phys. J. E* **2011**, 34, 56.

[39] V. Zaporojtchenko, T. Strunskus, K. Behnke, C. von Bechtolsheim, A. Thran, F. Faupel, *Microelectron. Engineer.* **2000**, 50, 465.

[40] G. Amarandei, C. O'Dwyer, A. Arshak, U. Thiele, U. Steiner, D. Corcoran, *Langmuir* **2013**, *29*, 6706.

[41] G. Amarandei, I. Clancy, C. O'Dwyer, A. Arshak, D. Corcoran, *ACS Appl. Mater. Interfaces*, **2014**, *6*, 20758.

[42] M. Schwartzkopf, A. Hinz, O. Polonskyi, T. Strunskus, F.C. Löhrer, V. Körstgens, P. Müller-Buschbaum, F. Faupel, S.V. Roth, *ACS Appl. Mater. Interfaces*, **2017**, *9*, 5629.

[43] I. Platzman, R. Brener, H. Haick, R. Tannenbaum, *J. Phys. Chem. C* **2008**, *112*, 1101.

[44] N.A. Mohemmed Shanid, M. Abdul Khadar, *Thin Sol. Films* **2008**, *516*, 6245.

[45] J. H. Kim, S. H. Ehrman, T. A. Germer, *Appl. Phys. Lett.* **2004**, *84*, 1278.

[46] A. Eskandari, P. Sangpour, M.R. Vaezi, *Mater. Chem. Phys.* **2014**, *147*, 1204.

Graphical Abstract

Polymer films with metal nanoparticles are of interest for applications in electronics, optics, sensing as well as in biological and medical branches. We present an approach on controlling the extent of metal nanoparticle embedding into polymer films and results of systematic study on dynamics of this process as a function of particles size, annealing temperature and type of polymer.